Crystal structure of NiO under high pressure

T. Eto and S. Endo
Research Center for Materials Science at Extreme Conditions, Osaka University, Toyonaka, Osaka 560-8531, Japan

M. Imai
National Research Institute for Metals, Tsukuba, Ibaraki 305-0047, Japan

Y. Katayama
Japan Atomic Energy Research Institute, Mikazuki, Sayo, Hyogo 679-5198, Japan

T. Kikegawa
Institute of Materials Structure Science, High Energy Accelerator Research Organization, Tsukuba, Ibaraki 305-0801, Japan
(Received 30 August 1999; revised manuscript received 28 January 2000)

The effect of pressure on the lattice parameters of NiO with a rhombohedral distorted $B1$ structure was investigated up to 141 GPa by *in situ* angle-dispersive x-ray diffraction using synchrotron radiation, an imaging plate, and a diamond anvil cell. The lattice constants a and c, expressed in the hexagonal lattice, decrease monotonically with increasing pressure. The axial ratio c/a also decreases monotonically with increasing pressure, indicating that the distortion in the rhombohedral [111] direction becomes larger as pressure increases. No phase transition was observed up to 141 GPa. A significant change of pressure coefficient of c/a above 60 GPa, as suggested by a recent theoretical calculation, was not observed.

I. INTRODUCTION

The investigation of the behavior of transition-metal monoxides under high pressure is very important from two viewpoints, namely, the interests in an antiferromagnetic Mott-type insulator in solid-state physics and in their roles in the deep part of the Earth in geophysics. NiO is an antiferromagnetic Mott-type insulator with a Néel temperature (T_N) of 523 K. Above T_N, NiO has a cubic rocksalt ($B1$) structure. Below T_N, the magnetic moments are aligned ferromagnetically on the (111) plane along one of the $[11\bar{2}]$ directions of the cubic cell, and the moments between the adjacent planes are coupled antiferromagnetically with each other.[1,2] As a result, the cubic cell is distorted slightly in the direction of the antiferromagnetic ordering and becomes a contracted rhombohedral cell.[3] No pressure-induced structural phase transition was observed in NiO, although several groups have conducted high-pressure experiments by static compression up to 28 GPa (Ref. 4) and by shock compression up to 147 GPa.[5] This is in contrast to the results in $3d$ transition-metal monoxides such as MnO,[6,7] FeO,[8–10] and CoO,[11] in which structural phase transitions were observed at high pressures.

Recently, the total energies of the distorted $B1$ and $B2$ (cesium-chloride) structures of NiO were calculated within the density-functional formalism by the local-spin-density approximation (LSDA) using an optimized pseudopotential method by Sasaki.[12] This calculation predicted that the pressure coefficient of the axial ratio c/a, $-d(c/a)/dP$, increases at around 60 GPa, indicating the enhancement of the lattice distortion by pressure, and that the first-order phase transition from the distorted $B1$ to $B2$ structure occurs at 318 GPa and is accompanied by metallization. However, details of the pressure effect on the lattice constants above 28 GPa by static compression have not been experimentally reported yet. In this study, we measured the pressure dependence of the lattice constants of NiO up to 141 GPa for a comparison with theoretical results.

II. EXPERIMENT

The specimen of NiO powder purchased from CERAC was of 99.995% nominal purity. The lattice constants under ambient conditions were determined by x-ray powder diffraction using Co $K\alpha$ radiation. The obtained lattice constants are $a=2.955\,92(5)$ Å and $c=7.2294(1)$ Å for the hexagonal description of the rhombohedral cell.[13] The resulting axial ratio is $c/a=2.4457(1)$. This value is smaller than the c/a ratio for the $B1$ structure, $\sqrt{6}=2.4495$, which indicates that the $B1$ lattice contracts in the [111] direction due to antiferromagnetic ordering, as mentioned above.

The crystal structure of NiO under high pressure was studied by *in situ* angle-dispersive x-ray diffractometry using monochromatized synchrotron radiation and an imaging plate at the Photon Factory (Beam Line 18C) of the Institute of Materials Structure Science (run A), and at SPring-8 (Beam Line 10XU) of the Japan Synchrotron Radiation Research Institute (run B). High pressure was generated with a diamond anvil cell (DAC). Diamonds of 400 μm culet diameter with a central flat region of 200 μm diameter and a bevel angle of 7° were used. The opening angle of the backing plate for diffraction was limited to $-35° \leqslant 2\theta \leqslant +35°$. Powder NiO was filled together with a 4:1 methanol-ethanol mixture in a hole of 50 μm diameter of a preindented gasket of 30–35 μm thickness. Helium was not used in the present experiment as a pressure medium because megabar generation with it was technically difficult, although it is suitable to maintain the sample under a hydrostatic condition. A small amount of ruby powder was also enclosed as a pressure marker in the gasket hole. Other experimental conditions are listed in Table I. In run B, x rays were irradiated on the part

TABLE I. Experimental conditions in the present x-ray study.

Run No.	Collimator size in diameter (μm)	Gasket material	Pressure determination	Maximum pressure (GPa)	Wavelength of x ray (Å)
Run A (Photon Factory)	25, 40	Stainless steel	Ruby fluorescence	81.9	0.6196
Run B (SPring-8)	40	Rhenium (Re)	EOS of Re	141.7	0.6199

of the sample slightly closer to the edge of the rhenium (Re) gasket in order to determine the lattice constants of the Re gasket at the same time; the pressure was obtained from the equation of state (EOS) of Re established by Vohra *et al.*,[14] because the ruby fluorescence disappeared above 80 GPa in the present experiment.

III. RESULTS

Figure 1(a) shows x-ray diffraction patterns for various pressures in run A, in which the pressure was determined by the ruby fluorescent technique. In the figure, the diffraction peaks are indexed as a hexagonal system. Under ambient conditions, the deviation from the $B1$ structure is relatively small: the rhombohedral angle, which is 60° for an undistorted cell, is 60.08° under ambient conditions.[15] As a result, a few peaks overlapped into a single profile, as shown in Fig. 1(a). With increasing pressure, the positions of diffraction peaks shift to higher angles, and the peak widths become broader. The absolute values of the widths are assumed to increase with pressure due to the increase of nonhydrostaticity of the pressure medium. This nonhydrostaticity effect is expected to be removed by dividing the widths with that of the 012 peak. The widths of the overlapping peaks 101 +003, 110+104, and 021+113+015 become broader with increasing pressure, even when compared with the 012 peak width. With increasing lattice distortion, the gap between diffraction peaks in a overlapping peak becomes wider, and the overlapped peak becomes broad. Therefore, the broadening of the overlapped peaks indicates the enhancement of lattice distortion by pressure. Figure 2(a) shows several x-ray diffraction patterns for various pressures obtained in run B. The crosses and asterisks show diffraction peaks from a collimator and Re gasket, respectively. A few peaks diffracted from the collimator were not eliminated due to a trivial mistake in the setup in run B: they originated probably from the Pt tip of the collimator. Figure 2(b) shows the pattern in which the peaks of the Re gasket are dominant. The pressures determined by the EOS of Re (Ref. 14) in the case that x rays were irradiated on the edge of a Re gasket [Fig. 2(b)] were 3–5 GPa lower at around 100 GPa than those in the case that x rays were irradiated on the part of the sample slightly closer to the gasket [Fig. 2(a)]. The pressures determined from the weak diffraction lines of Re in the latter case were adopted as the pressures of the sample in run B. However, they are not the exact pressures of the sample at the center of the gasket. In the diffraction patterns of Fig. 2(b), no significant change was observed even at the highest pressure, 141 GPa.

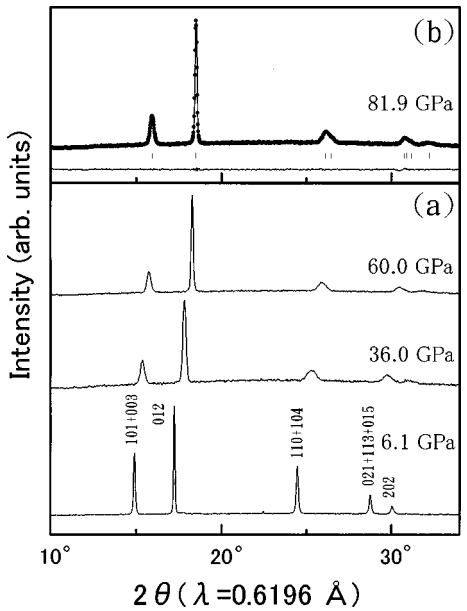

FIG. 1. (a) X-ray diffraction patterns of NiO at various pressures at room temperature (run A). The observed patterns are indicated by the solid lines. (b) WPPD analysis result for NiO at 81.9 GPa. The observed pattern is indicated by the dots, and the fitting function and their difference (bottom) are indicated by solid curves.

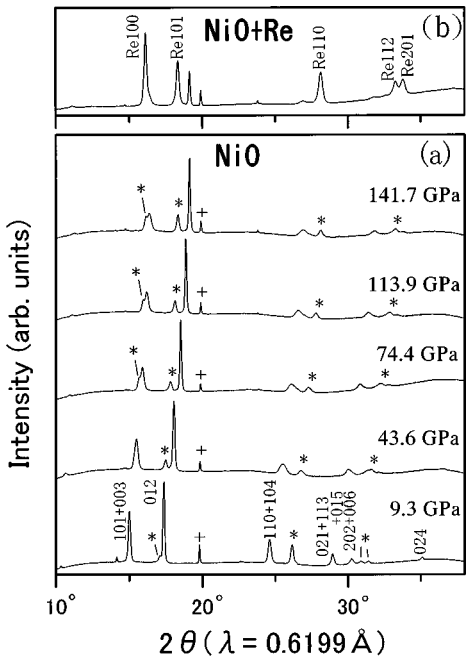

FIG. 2. (a) X-ray diffraction patterns of NiO at various pressures at room temperature (run B). The crosses and asterisks denote the diffraction peaks from a collimator and a Re gasket, respectively. (b) A pattern obtained by irradiating x ray on the edge of a Re gasket hole at 141.7 GPa.

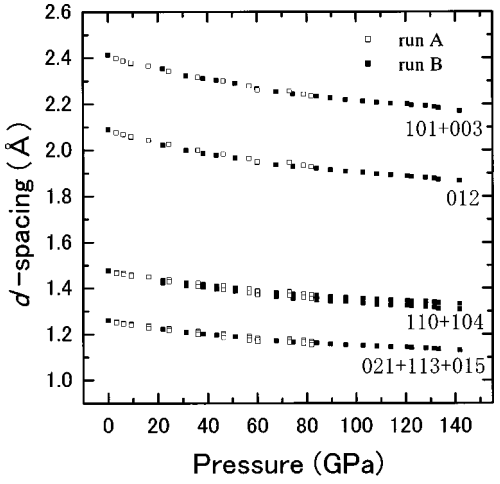

FIG. 3. Pressure dependence of d spacings of NiO.

The data for run A were analyzed by the whole-powder-pattern decomposition (WPPD) method.[16] Figure 1(b) shows an example of the fitting results; the dots indicate the observed pattern, the solid curve the fitting function, and their difference is shown at the bottom by the solid curve. These fittings seem adequate even at the highest pressures of run A. For the data analysis of run B, the Gaussian function was fitted to the observed diffraction peaks of NiO, 101, 012, 110+104, and the lattice constants were determined by the least-squares method. For the overlapping peak of 110 +104, two Gaussian curves were adopted to decompose it into two peaks. Figure 3 shows the pressure dependence of the d spacing. The overlapping peak 110+104 splits into 2 with pressure, which suggests that the distortion in the [111] direction of the rhombohedral cell becomes large with increasing pressure. There is, however, no remarkable change in Figs. 1, 2, and 3, which clearly indicates that no structural phase transition occurred up to 141 GPa, the maximum pressure used in this experiment.

The pressure dependences of the lattice parameters a and c are shown in Figs. 4(a) and 4(b), together with the calculated curves by Sasaki.[12] The experimental behaviors are similar to the calculated results up to 50 GPa, but become markedly different above 50 GPa, especially for the lattice constant a. In the experiment, the lattice constant a decreases monotonically with increasing pressure, while in the calculation, it exhibits nonmonotonic behavior with increasing pressure: it decreases below 120 GPa and increases above 120 GPa. Figure 4(c) shows the axial ratio of c/a as a function of pressure, together with the calculated result.[12] The axial ratio c/a decreases with pressure, which indicates that the deviation from the c/a value of the $B1$ structure becomes larger. The pressure coefficient of c/a, $d(c/a)/dp$, is almost constant over the entire pressure region in the experiments, while $-d(c/a)/dp$ becomes larger above 60 GPa in the calculation. The difference in the c/a behavior between the experiment and the calculation reflects, of course, the difference in the pressure dependences of lattice constants a and c.

Figure 5 shows the volume of a hexagonal unit cell as a function of pressure, together with the data of static compression without a gasket by Huang[4] and of shock compression by Noguchi *et al.*[5] The present results are in good agreement with previous data, although a slight difference from the

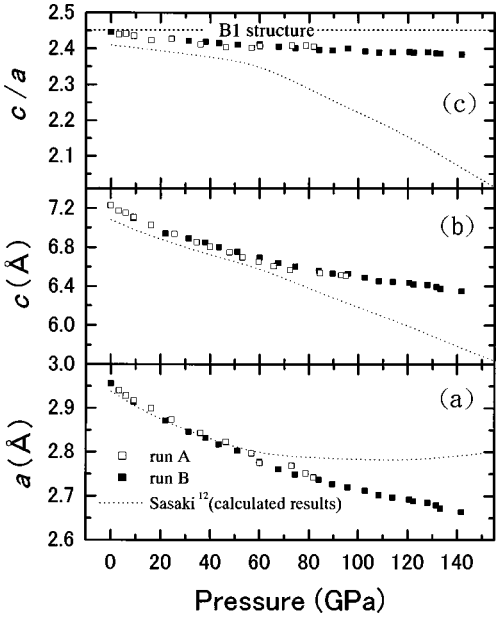

FIG. 4. Pressure dependence of the lattice parameters of NiO: (a) the lattice constant a, (b) the lattice constant c, and (c) the axial ratio c/a. The error bars are within the symbols. The dotted curves indicate the calculated results by Sasaki (Ref. 12). The dashed line in (c) indicates the c/a ratio for the $B1$ structure.

shock data can be observed at high pressure above 110 GPa. The following three factors are considered to be responsible for the discrepancy: (i) the exact pressure of the sample may be slightly different from the value determined from the EOS of the Re gasket in the present experiment as mentioned above, (ii) the nonhydrostaticity due to using an alcohol mixture may be a part of the reason as described later, and (iii) a magnetic transition such as that predicted by the first-principles computation using the generalized-gradient approximation[17] (GGA) might occur at around 110 GPa at

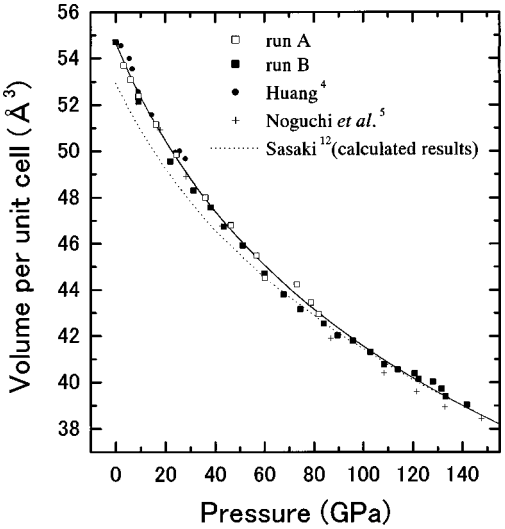

FIG. 5. Pressure dependence of the unit cell volume of NiO. The error bars are within the symbols. The fitting function of Birch-Murnaghan EOS to the experimental result is indicated by the solid line. The values by static [Huang (Ref. 4)] and shock [Noguchi *et al.* (Ref. 5)] compression are indicated by a solid circle and a cross, respectively. The dotted curve indicates the calculated results by Sasaki (Ref. 12).

TABLE II. Bulk modulus B_0 and its pressure derivative B_0' of NiO.

Researchers	B_0 (GPa)	B_0'	Pressure range (GPa)	Method
Clendenen and Drickamer[a]	199	4.1	0–27.5	Drickamer cell
Wakabayashi *et al.*[b]	186	4.0	0–8.0	Drickamer cell
Noguchi *et al.*[c]	191	3.9[d]	0–147.6	Shock wave
Manghnani *et al.*[e]	208	5.0	0–24.0	DAC (alcohol mixture)[f]
Huang[g]	187(7)	4.0	0–6.6	DAC (alcohol mixture)[f]
Present work	192(4)	4.0	0–9.3	DAC (alcohol mixture)[f]
	203(2)	4.0	0–60.1	
	210(2)	4.0	0–141.7	
Sasaki[h]	236	4.28	0–60	LSDA calculation

[a]Reference 21.
[b]Reference 22.
[c]Reference 5.
[d]The third-order Birch-Murnaghan EOS with $B_0''=-0.03\,\mathrm{GPa}^{-1}$.
[e]Reference 23.
[f]A diamond anvil cell using an alcohol mixture as a pressure medium.
[g]Reference 4.
[h]Reference 12.

room temperature in the present experiment. There is a relatively good consistency between the calculated p-V curve and the experimental ones at higher pressures, but it is considered to be an accidental result when the large discrepancy of the lattice constant at this pressure region shown in Fig. 4 is taken into account. The lattice constants determined by the calculation are different from the experimental values even under ambient pressure. This comes from the difficulty in the band calculation of the transition-metal oxides, as discussed later.

The bulk modulus B_0 is determined by fitting the P-V data to the second-order Birch-Murnaghan (Ref. 18) EOS assuming $B_0'=4$, where B_0' is the pressure derivative of B_0 at zero pressure. Since the experimental value of B_0 is known to depend on the pressure range to be fitted,[19,20] B_0 is determined in three pressure regions: a low-pressure region from 0 to 9.3 GPa, the pressure region from 0 to 60.1 GPa, and the entire pressure region up to 141.7 GPa. The values of B_0 and B_0' are listed in Table II together with previously reported ones. Huang's value in the table was determined under hydrostatic conditions with a gasket.[4] The present value of $B_0=192(4)$ GPa, determined in the low-pressure region, agrees with those by Wakabayashi *et al.*[22] and Huang which were obtained in a relatively low-pressure region. The B_0 value becomes larger when data obtained at higher pressures are fitted. The present value of $B_0=216(3)$ GPa determined in the entire pressure region is about 20% larger than that in the low-pressure region. Huang pointed out that the value of the bulk modulus obtained under nonhydrostatic conditions tends to be higher than that under hydrostatic conditions, because of the shear stress.[4] Therefore, the shear stress induced by nonhydrostaticity is one of the reasons why B_0 determined in the low-pressure region is smaller than that in the entire pressure region. This consideration may also explain why the volume in the present study in Fig. 5 is slightly larger than the corresponding shock compression values by Noguchi *et al.*[6] at high pressures.

IV. DISCUSSION

In the present study, no structural phase transition from a distorted $B1$ structure was observed up to 141 GPa. This is consistent with the results of the shock compression experiment up to 147 GPa.[5] Many materials with $B1$ structure, such as CaO,[24] SrO,[25] and BaO,[26] undergo a pressure-induced phase transition to the $B2$ structure. For this reason, the transition pressure for the $B1$ to $B2$ transition was also discussed for NiO. Noguchi *et al.*[5] considered that the $B1$ phase was very stable for the $B1$ to $B2$ transition on the basis of three facts: (i) the transition pressure increases with decreasing cationic ion radius in alkaline-earth metal monoxides, (ii) MgO, which has the smallest cationic radius, still remains in the $B1$ phase up to 227 GPa,[27] and (iii) the cationic radius of the Mg^{2+} ion is larger than that of the Ni^{2+} ion. The LSDA calculation result predicted a transition pressure of 318 GPa for the distorted $B1$ to $B2$ transition in NiO.[12] This value is much higher than the highest pressure in the present experiments, 141 GPa. In $3d$ transition-metal monoxides such as MnO,[6,7] FeO,[8–10] and CoO,[11] pressure-induced phase transitions were observed in the megabar range. In MnO, the high-pressure phase over 120 GPa has a normal NiAs-type ($B8$) structure.[7] In FeO, the $B8$ structure was reported to appear at pressures above 70 GPa by heating above approximately 900 K.[10] Fang *et al.*[28] performed a first-principles calculation for FeO and MnO under high pressure and indicated that the high-pressure phase of MnO is the normal $B8$ structure, while that of FeO is the inverse $B8$ structure ($iB8$). Their analysis of x-ray diffraction experiments provided further support for the theoretical prediction for both FeO and MnO. However, the phase transition to $B8$-related structures in NiO has not yet been theoretically discussed.

The effect of pressure on the structure of NiO obtained in the present study is different from that calculated above 50 GPa, as shown in Figs. 4 and 5. In the calculation, the volume dependence of rhombohedral distortion was analyzed by

expanding the total energy with respect to the shear strain ε up to the fourth-order term and determining the coefficient of each term.[12] The analysis reveals that a coefficients of the second-order term of ε, $b(V)$, shows significant volume dependence and that the rhombohedral distortion is governed mainly by the behavior of the second-order term. The second-order term $b(V)\varepsilon^2$ functions as the restoring force for the distortion when $b(V)$ has a positive value. Here $b(V)$, which has a positive value near 0 GPa, decreases with pressure and has negative values above 120 GPa. Then the elasticity term $b(V)\varepsilon^2$ no longer functions as the restoring force for the distortion, and finally, large lattice distortion occurs. As a result, $-d(c/a)/dp$ becomes larger above 60 GPa. Thus a negative value of $b(V)$ is the reason why c/a decreases steeply with pressure above 60 GPa. This behavior of the c/a ratio is not seen in the experimental results, as shown in Fig. 4(c). Here $b(V)$ is contributed by the electrostatic energy (b_{es}) and the band-structure energy (b_{bs}); b_{es} has a negative value and b_{bs} a positive one over the entire pressure range considered in the calculation. Therefore, a negative value of $b(V)$ at a small volume indicates an overestimation of $-b_{es}$ or an underestimation of b_{bs} in the calculation. Since b_{es} can be more strictly defined than b_{bs}, the LSDA probably underestimates b_{bs}.

Regarding the value of B_0, 236 GPa, in the LSDA calculation determined from the pressure range of 0–60 GPa (Ref. 12) is about 16% larger than 203(2) GPa in the present study from the range of 0–60.1 GPa listed in Table II. Recently, a calculation with the GGA for NiO was performed,[29] which gives a value of B_0 close to the experimental one. But it gives almost the same result with respect to the behavior of c/a as the LSDA calculation.[12] It is likely that the band calculation of the transition-metal oxides is difficult, considering the fact that the stable structure of FeO at zero pressure cannot be obtained even by the GGA.[28] The discrepancy between the experiment and calculation mainly results from the difficulty in describing the $3d$-electron correlation of a Mott-type insulator precisely. This is the reason for the large discrepancy between the lattice constants of the present experiment and the theory[12] in NiO.

V. CONCLUSION

The pressure dependences of the lattice constants of NiO were determined up to 141 GPa by *in situ* x-ray diffraction. The lattice constants a and c (expressed in the hexagonal lattice) decrease monotonically as pressure increases. The value of c/a also decreases monotonically, which indicates that the rhombohedral distortion is enhanced by pressure, but the c/a behavior is different from that of previous calculations. This difference may be attributed to the underestimation of the band-structure energy in the calculation.

ACKNOWLEDGMENTS

We are grateful to Dr. T. Sasaki (the author of Ref. 12), National Research Institute for Metals, for valuable comments and discussions. We thank Dr. S. Morimoto, Graduate School of Engineering Science, Osaka University, for conducting the experiment under ambient conditions and for useful comments. This work was supported by CREST (Core Research for Evolutional Science and Technology) of JST (Japan Science and Technology Corporation), and was performed under proposal No. 96G131 and No. 98G076 of the Photon Factory and No. 1999A0259-ND-np of SPring-8.

[1] C. G. Shull, W. A. Strauser, and E. O. Wollan, Phys. Rev. **83**, 333 (1951).
[2] J. Baruchel, M. Schlenker, K. Kurosawa, and S. Saito, Philos. Mag. B **43**, 853 (1981).
[3] H. P. Rooksby, Acta Crystallogr. **1**, 226 (1948).
[4] E. Huang, High Press. Res. **13**, 307 (1995).
[5] Y. Noguchi, M. Uchino, H. Hikosaka, T. Atou, K. Kusaba, F. Fukuoka, T. Mashimo, and Y. Syono, J. Phys. Chem. Solids **60**, 509 (1999).
[6] Y. Noguchi, K. Kusaba, K. Fukuoka, and Y. Syono, Geophys. Res. Lett. **23**, 1469 (1996).
[7] T. Kondo, T. Yagi, Y. Syono, T. Kikegawa, and O. Shimomura, Rev. High Pressure Sci. Technol. **7**, 148 (1998).
[8] R. Jeanloz and T. J. Ahrens, Geophys. J. R. Astron. Soc. **62**, 505 (1980).
[9] T. Yagi, T. Suzuki, and S. Akimoto, J. Geophys. Res. **90**, 8784 (1985).
[10] Y. W. Fei and H. K. Mao, Science **266**, 1678 (1994).
[11] Y. Noguchi, T. Atou, T. Kondo, T. Yagi, and Y. Syono, Jpn. J. Appl. Phys., Part 2 **38**, L7 (1999).
[12] T. Sasaki, Phys. Rev. B **54**, R9581 (1996).
[13] *International Tables for Crystallography*, edited by T. Hahn (Kluwer Academic, Dordrecht, 1995), Vol. A, pp. 12–14 and 63–64.
[14] Y. K. Vohra, S. J. Duclos, and A. L. Ruoff, Phys. Rev. B **36**, 9790 (1987).
[15] C. J. Toussaint, J. Appl. Crystallogr. **4**, 293 (1971).
[16] H. Toraya, J. Appl. Crystallogr. **19**, 440 (1986).
[17] R. E. Cohen, I. I. Mazin, and D. G. Isaak, Science **275**, 654 (1997).
[18] J. R. Macdonald and D. R. Powell, J. Res. Natl. Bur. Stand., Sect. A **75**, 441 (1971).
[19] O. Schulte and W. B. Holzapfel, Phys. Rev. B **53**, 569 (1996).
[20] K. Takemura, Phys. Rev. B **56**, 5170 (1997).
[21] R. L. Clendenen and H. G. Drickamer, J. Chem. Phys. **44**, 4223 (1966).
[22] I. Wakabayashi, H. Kobayashi, H. Nagasaki, and S. Minomura, J. Phys. Soc. Jpn. **25**, 227 (1968).
[23] M. H. Manghnani, L. J. Wang, S. Usha-Devi, and L. C. Ming, EOS, Trans. Am. Geophys. Union **73**, 579 (1992).
[24] P. Richet, H. K. Mao, and P. M. Bell, J. Geophys. Res. **93**, 15 279 (1988).
[25] L. Liu and W. A. Bassett, J. Geophys. Res. **78**, 8470 (1973).
[26] L. Liu and W. A. Bassett, J. Geophys. Res. **77**, 4934 (1972).
[27] T. S. Duffy, R. J. Hemley, and H. K. Mao, Phys. Rev. Lett. **74**, 1371 (1995).
[28] Z. Fang, K. Terakura, H. Sawada, T. Miyazaki, and I. Solovyev, Phys. Rev. Lett. **81**, 1027 (1998).
[29] T. Sasaki (private communication).